Electronic Supplementary Material (ESI) for Analyst.

Supporting Information

Design of a photoelectrochemical lab-on-a-chip immunosensor based on enzymatic production of quantum dots in situ

Beatriz Díez-Buitrago[a,b], Francisco Javier Fernández-SanArgimiro[b], Jaione Lorenzo[b], Goran Bijelic[b], Nerea Briz[b], Valeri Pavlov[a*]

[a] CIC biomaGUNE, Paseo Miramón 182, 20014 Donostia-San Sebastián, Spain

[b] Tecnalia, Basque Research and Technology Alliance (BRTA), Paseo Mikeletegi 2, 20009 Donostia-San Sebastián, Spain

† Corresponding author: e-mail: vpavlov@cicbiomagune.es. Telephone: +34 943 00 53 08

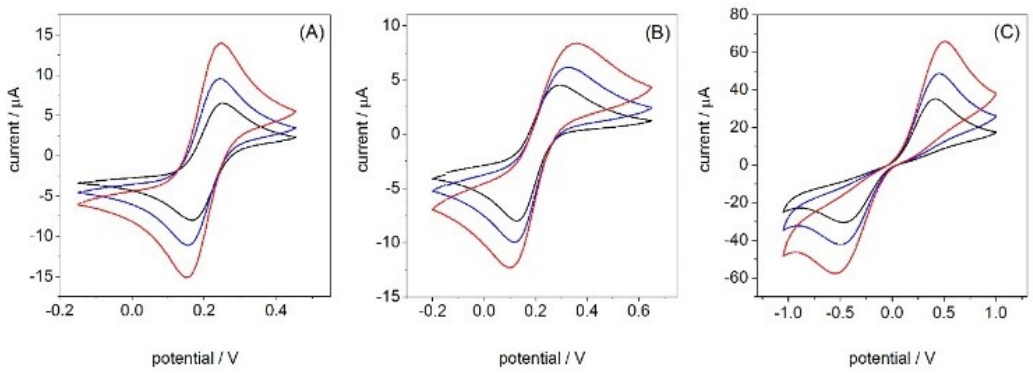

Figure S1. Cyclic voltammograms of (a) commercial SPCE, (b) home-made SPCE on PS 190 µm and (c) home-made SPCE on PS 1.2 mm in the presence of potassium ferro/ferrihexacyanide 5 mm in PB 10 mm ph 7.4, scan rate 50 mv s^{-1} (black), 100 mv s^{-1} (blue) and 200 mv s^{-1} (red).

Table S1. Comparison of various carbon electrodes with potassium ferro/ferrihexacyanide redox couple.

Electrode	Scan rate / mV s^{-1}	ΔEp / mV	I_{ox}/I_{red}
PS 190 µm	50	156	0.86
	100	181	0.85
	200	217	0.83
PS 1.2 mm	50	821	1.42
	100	871	1.41
	200	957	1.39
Commercial	50	76	0.92
	100	81	0.92
	200	81	0.91

Table S2. Parameters of equations obtained at various carbon electrodes under scan rate study.

Electrode	anodic			cathodic		
	k mA cm^{-2} / $mV^{1/2}$ $s^{-1/2}$	*q* mA cm^{-2}	R^2	*k* mA cm^{-2} / $mV^{1/2}$ $s^{-1/2}$	*q* mA cm^{-2}	R^2
PS 190 µm	0.376	3.050	0.992	0.484	3.215	0.993
PS 1.2 mm	2.441	11.743	0.998	1.676	9.210	0.990
Commercial	0.927	0.519	0.999	1.028	0.418	0.999

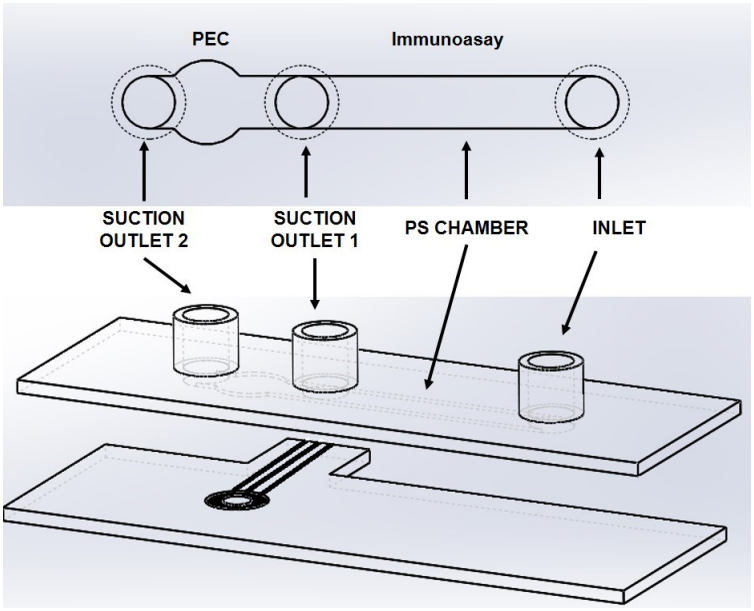

Figure S2. Top view of the design and dimensions of immunoassay (rectangle) and PEC (round) chambers. Lateral view of the inlets and outlets.

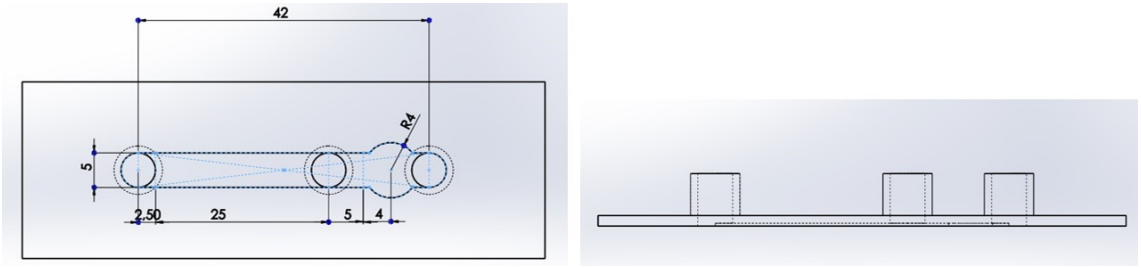

Figure S3. PS microfluidic layout consisting of a PS cover including the channel and the inlets/outlets and a bottom side made of aminated PS with integrated SPCE.

To prove that no unspecific binding to the surface is happening, thus preventing potential interferences caused by the presence of other proteins in the sample, the following study was performed: the detection antibody (biotinylated mouse anti-HSA antibody) was immobilised in aminated polystyrene surface followed by the addition of BSA 1% solution in PBS only in half of the samples (n=4), whereas the rest of samples were left unblocked (n=4). After a washing step, Streptavidin – ALP is added to all the samples and the rest of the protocol is applied unvaried as described in the manuscript to generate the CdS QDs and measure the PEC signal.

The results, as shown in the table below, prove that Streptavidin – ALP is nonspecifically adsorbed to the aminated polystyrene surface when the blocking step is skipped, leading to the formation of CdS QDs that produce a high current jump. However, when the surface is blocked with BSA 1%, the signal decreases significantly since only those Streptavidin – ALP molecules that bind specifically to the biotinylated antibodies lead to the formation of CdS QDs, thus reducing the observed current jump.

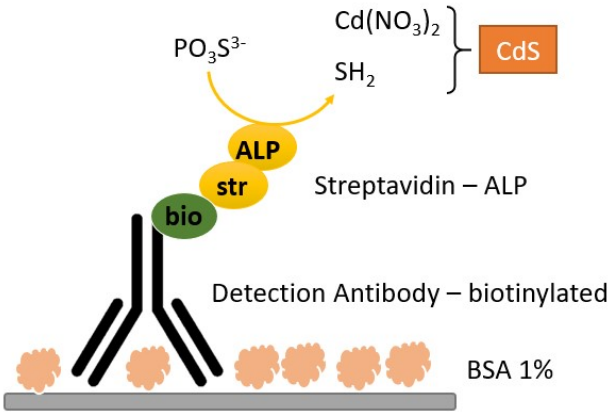

	ΔI / nA (n=4)
With BSA	54,0 ± 34
Without BSA	142,2 ± 28

Scheme S1. Strategy to demonstrate the absence of nonspecific binding upon BSA treatment.

On the other hand, there are plenty of examples in the literature using BSA as blocking agent, which prove the efficiency of this protein to block the surface and avoid unspecific binding of biomolecules in the microtiter well surface. Besides, the efficiency of BSA for blocking has been thoroughly characterised by Steinitz, preventing unspecific binding of alkaline phosphatase to both treated and non-treated plates when using BSA at concentrations equal or higher than 50 µg/mL (0.005% BSA) and up to 50 mg/mL (5% BSA) (Steinitz, 2000).

References

Steinitz, M., 2000. Anal. Biochem. 282 (2), 232–238.